JCZ: Zoologischer Anzeiger - A Journal of Comparative Zoology 313 (2024) 315–331

Contents lists available at ScienceDirect

Zoologischer Anzeiger

journal homepage: www.elsevier.com/locate/jcz

Discovery of a new Kinorhyncha species from the uncharted South Orkney Trench (Southern Ocean)

Nuria Sánchez [a,*], Marta García-Cobo [a,b], Mauricio Shimabukuro [b,c], Daniela Zeppilli [d], Hidetaka Nomaki [e], Alberto González-Casarrubios [a]

[a] Complutense University of Madrid (UCM), Faculty of Biology, Department of Biodiversity, Ecology and Evolution (BEE), Madrid, Spain
[b] Nordcee and HADAL, Department of Biology, University of Southern Denmark, Odense, Denmark
[c] Instituto de Oceanography, Universidade Federal do Rio Grande, Rio Grande, RS, Brazil
[d] Ifremer, Biologie et Ecologie des Ecosystèmes Marins Profonds, F-29280, Plouzané, France
[e] X-star, Japan Agency for Marine-Earth Science and Technology (JAMSTEC), Yokosuka, 237-0061, Japan

ARTICLE INFO

Handling Editor: Maikon Di Domenico

Keywords:
Kinorhynch
Taxonomy
Antarctic
Hadal
New species
Juveniles

ABSTRACT

The knowledge about the deep-sea Kinorhyncha community has increased considerably in recent years. However, the records of kinorhynchs inhabiting hadal depths are still extremely limited. In the present study, we describe a new species of *Echinoderes* discovered from the South Orkney Trench, Southern Ocean. *Echinoderes australis* sp. nov. is characterized by the presence of middorsal acicular spines on segments 4-8 and lateroventral ones on segments 6-9, and tubes in lateroventral position on segment 5, in lateral accessory position on segment 8, and in laterodorsal position on segment 10. Additionally, the new species has conspicuous papillary flaps on segments 8-9. Among its morphological characteristics, the increase in length of the middorsal spine of segment 8 and lateroventral spines of segment 9 in relation to those of the previous segments are striking features, showing a whip-like appearance. *E. australis* sp. nov. Becomes the third hadal species of the phylum. In addition, we provide morphological information on the two other species found in the trench. Finally, we study in detail the diversity and distribution patterns of the Kinorhyncha of the South Orkney Trench, addressing aspects such as species richness, abundance, number of adults versus juveniles and the effect of bathymetry on the community composition.

1. Introduction

Kinorhyncha is among the pool of neglected taxa for which less than 15 % of its estimated diversity is formally described (Appeltans et al., 2012; WoRMS Editorial Board, 2024). Their small size (0.1–1 mm) and the low number of taxonomists specialized in the group are likely behind this knowledge gap, as is also the case for other meiofaunal phyla (Lins et al., 2021). It should also be mentioned that knowledge of kinorhynch diversity is biased towards the most accessible ecosystems: of the nearly 350 described species, 73 were reported from deep-sea environments (>500 m depth according to Glover et al., 2024). From which, 27 species were found in the abyssal plain (3.000–6.000 m) (for the specific bibliography see e.g. Grzelak and Sørensen, 2022; Sánchez et al., 2022; González-Casarrubios et al., 2022) and only two species were properly identified from hadal depths (>6.000 m) (following Jamieson et al., 2010; Harris et al., 2014): *Echinoderes ultraabyssalis* Adrianov and Maiorova, 2019, from the Kuril-Kamchatka Trench; and *Echinoderes mamaqucha* Grzelak et al., 2021, from the Atacama Trench. The two echinoderms have a rather similar general appearance, which is not surprising since commonly in deep-sea environments speciation does not necessarily require morphological changes (Janssen et al., 2015).

Deep ocean trenches are hadal environments consisting of elongated basins formed by tectonic subduction or fault (United Nations Educational Scientific and Cultural Organization, 2009; Watling et al., 2013; Stewart and Jamieson, 2018). Trenches are typically characterized by very high pressure (increases by 1 atm/10 m) and low temperatures of restricted within-habitat variability (1–4 °C) (Jamieson et al., 2010). The scarcity of information on kinorhynch fauna from trenches makes this environment the least known in terms of biodiversity of the phylum.

Our investigation focuses on the South Orkney Trench (Southern Ocean), located between the Antarctic and southern temperate zones. The aim of the present contribution is to study the kinorhynch

* Corresponding author.
E-mail address: nurisanc@ucm.es (N. Sánchez).

https://doi.org/10.1016/j.jcz.2024.10.016
Received 29 August 2024; Received in revised form 23 October 2024; Accepted 25 October 2024
Available online 26 October 2024

community of the South Orkney Trench in terms of diversity and distribution patterns, and describe a new *Echinoderes* species from the trench.

2. Material and methods

2.1. Study site

The South Orkney trench is located in the Southern Ocean, approximately 200 km away from the South Orkney Islands, 800 km from the nearest coast of Antarctica and 1.600 km from South America. The deepest point of its axis reaches around 6.200 m deep (Vinogradova et al., 1993). The geographical position of the South Orkney Trench, in the center of the highly productive pelagic zone of the Southern Ocean, determines the rich and peculiar trophic structure of the bottom fauna down to the maximal depths (Vinogradova et al., 1993). This phenomenon is ensured by the trophic connections between the animals of the benthic and pelagic zones (Sokolova et al., 1996).

2.2. Sampling, extraction and preparation of specimens

The samples were collected in December 2019 during the research cruise KH-19-6_leg4 on board of the R/V *Hakuho-Maru* (JAMSTEC). Meiofauna was obtained using a multi-core (MUC) at two sampling sites of the South Orkney Trench: one site from the terrace (5.251 m depth) in the trench slope (A5200), and one site from the axis (6.271 m depth) of the trench (A6200) (Fig. 1). From each location (axis and terrace) three pseudo-replicates (from three different cores) were collected from the same MUC deployment. Sediment samples were sliced on board every one centimetre down to five centimetre and subsequently fixed in formalin 10 %.

Meiofauna was extracted using Ludox® HS-40 flotation method (Somerfield and Warwick, 1996) followed by a centrifugation at 3.000 rpm for 10 min. The Ludox extraction was repeated three times to guarantee better efficiency of the extraction. After Ludox extraction, the suspended solution was washed in 20 μm net, stained with Bengal Rose and preserved on ethylene glycol 20 %.

Kinorhyncha specimens were sorted under a stereomicroscope and prepared for microscopy study. For light microscopy (LM), adult specimens were passed through a graded series of glycerine, kept overnight in a solution of 100 % glycerine and mounted on glass slides using dimethyl hydantoin formaldehyde resin (DMHF). Subsequently, specimens were photographed and identified to species level using the interactive identification key made by Yamasaki et al. (2020) and an Olympus© BX51-P differential interference contrast microscopy with an Olympus© DP-70 camera. Measurement of the specimens was done according to the standardized criteria in González-Casarrubios et al. (2023). Total measurements of the new species are compiled in the additional material (Supplementary Table S1) and uploaded to the Kinorhyncha Measurement Database (González-Casarrubios and Yamasaki, 2022). For scanning electron microscopy (SEM), adult specimens were passed through a graded series of ethanol, then through a graded series of acetone, and critical-point dried. Finally, specimens were mounted on aluminium stubs and sputter-coated with gold-palladium for 90s for examination with a JEOL© JSM-6335F field emission scanning electron microscope at the ICTS Centro Nacional de Microscopía Electrónica (Complutense University of Madrid, Spain).

Adobe® Photoshop and Illustrator 2023 software were used for the line art illustrations and image compositions. Plots were performed in R v.1.1.453 (R Core Team, 2021) using the ggplot2 package (Fox and Weisberg, 2019). Type material of the new species was deposited at the Natural History Museum of Denmark (NHMD).

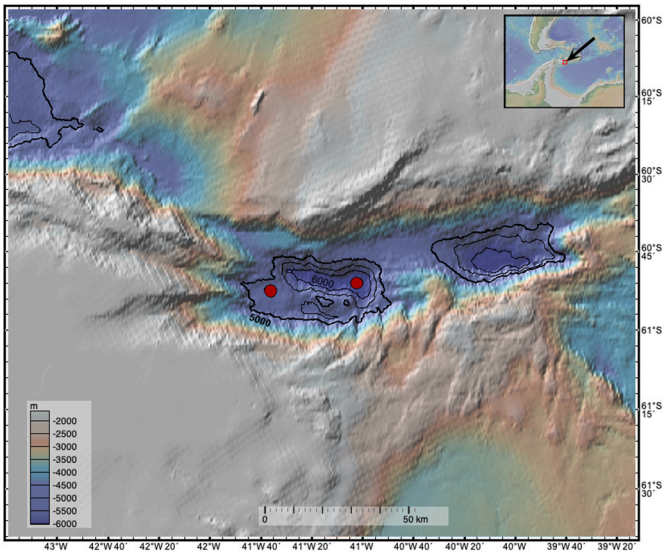

Fig. 1. Map showing the location of the study site in the South Orkney Trench, Southern Ocean.

3. Results

3.1. Taxonomic account

Class Cyclorhagida (Zelinka, 1896) *sensu* Herranz et al., 2022.
Order Echinorhagata Sørensen et al., 2015.
Family Echinoderidae Carus, 1885.
Genus *Echinoderes* Claparède, 1863

Echinoderes australis sp. nov.

urn:lsid:zoobank.org:pub:60C568A3-C443-428D-878F-89BAACBE6E31

(Figs. 2–5, Tables 1 and 2).

3.1.1. Synonymy

Echinoderes sp. 2 (in Grzelak et al., 2021).

3.1.2. Material examined

Type material: Holotype, adult female, collected in 2019/12/19 at South Orkney Trench, Southern Ocean: Station A6200; Coordinates 60° 51′ 1.200″S, 41° 2′ 13.800″ W; at 6.271 m depth; mounted in DMHF, deposited at NHMD under catalogue number: NHMD-1784619. Paratypes, 2 adult males and 1 adult female, same collecting data as holotype; mounted in DMHF, deposited at NHMD under catalogue numbers: NHMD-1784620 to NHMD-1784622. An additional male paratype, collected in 2019/12/19 at South Orkney Trench, Southern Ocean: Station A5200; Coordinates 60° 52′ 30.000″ S, 41° 36′ 2.400″ W; at 5.251 m depth; mounted in DMHF, deposited at NHMD under catalogue number: NHMD-1784623.

Non-type material: 2 adult females, same collecting data as holotype, mounted for SEM examination, deposited at the meiofaunal laboratory of the UCM. 1 adult female (broken), same collecting data as holotype, mounted in DMHF, deposited at the meiofaunal laboratory of the UCM.

3.1.3. Diagnosis

Echinoderes with middorsal acicular spines on segments 4-8 and lateroventral ones on segments 6-9, both increasing in length on posterior segments. Very long middorsal spine of segment 8 and lateroventral spines of segment 9, with whip-like appearance. Paired large tubes in lateroventral position on segments 5, in lateral accessory position on segment 8, and in laterodorsal position on segment 10. Conspicuous middorsal papillary flaps on segments 8-9.

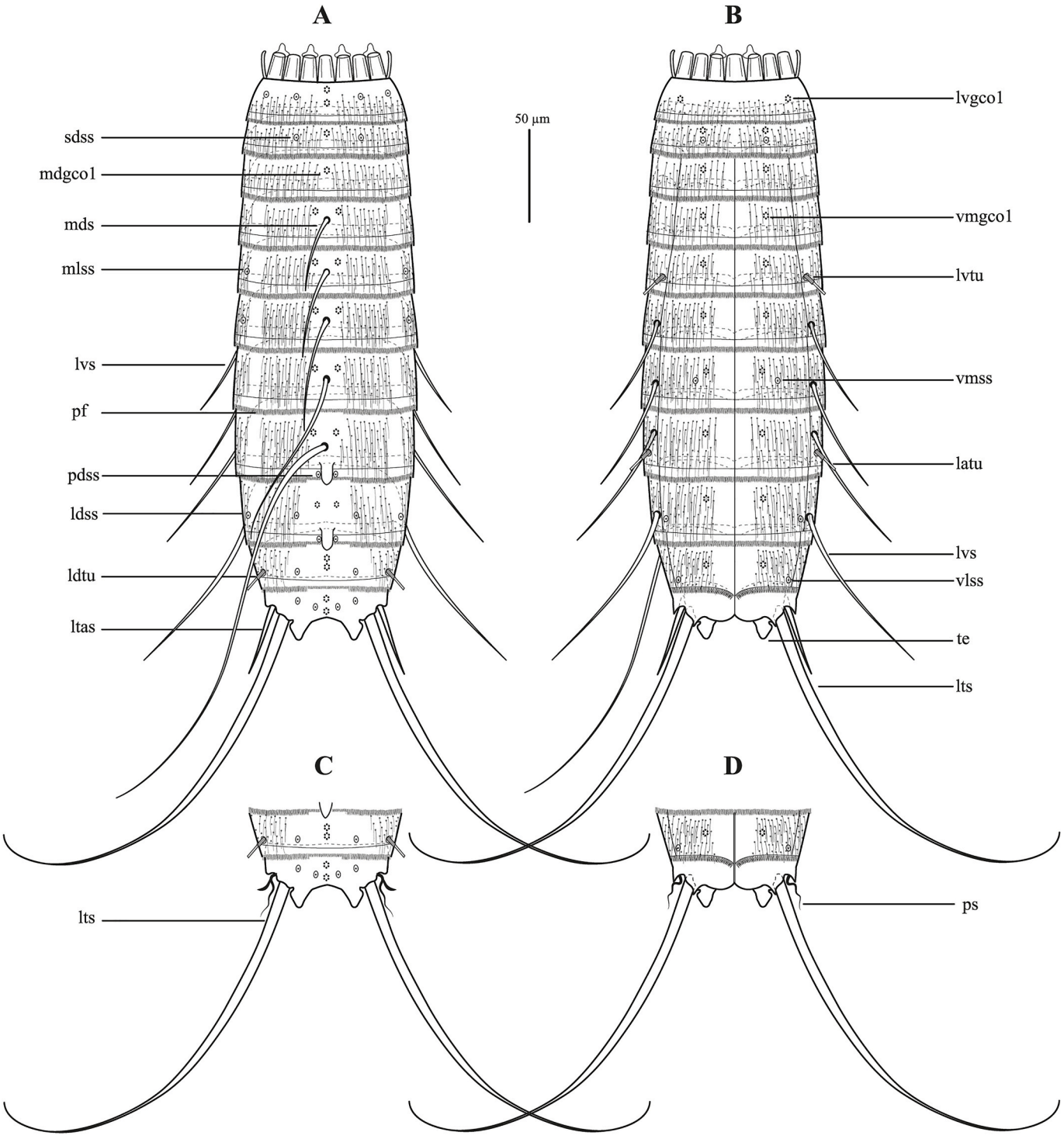

Fig. 2. Line art drawing of *Echinoderes australis* sp. nov. based on type material. A: Dorsal female overview; B: Ventral female overview; C: Dorsal male view of segments 10–11. D: Ventral male view of segments 10–11. Abbreviations: latu, lateral accessory tube; ldss, laterodorsal sensory spot; ldtu, laterodorsal tube; ltas, lateral terminal accessory spine; lts, lateral terminal spine; lvgco1, lateroventral type 1 glandular cell outlet; lvs, lateroventral spine; lvtu, lateroventral tube; mdgco1, middorsal type 1 glandular cell outlet; mds, middorsal spine; mlss, midlateral sensory spot; pdss, paradorsal sensory spot; pf, papillary flap; ps, penile spine; sdss, subdorsal sensory spot; te, tergal extension; vlss, ventrolateral sensory spot; vmgco1, ventromedial type 1 glandular cell outlet; vmss, ventromedial sensory spot.

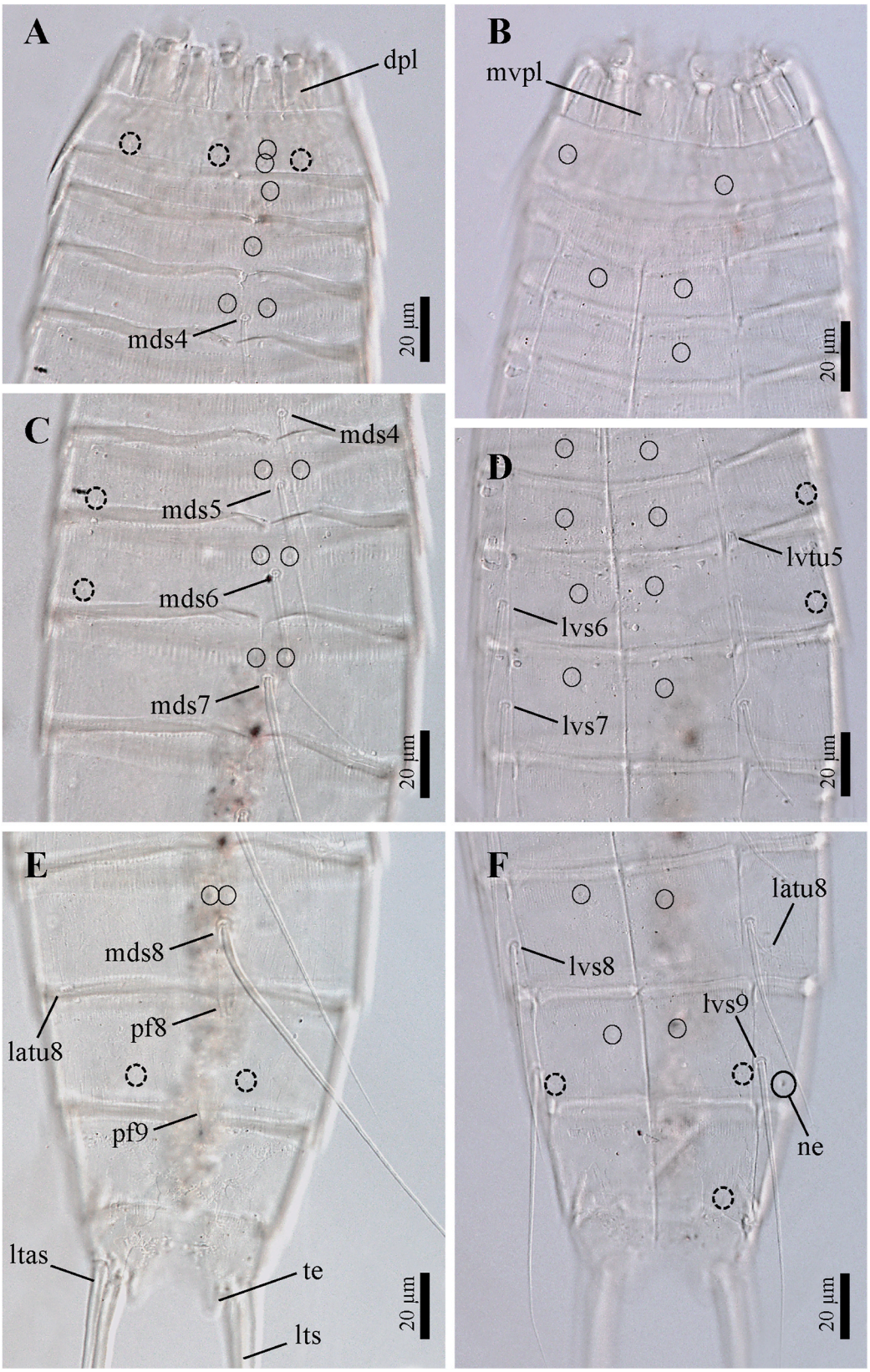

Fig. 3. Light micrographs of female holotype NHMD-1784619 of *Echinoderes australis* sp. nov., showing details on the neck and segments 1–11. A: Dorsal view on the neck and segments 1–4; B: Ventral view on the neck and segments 1–4; C: Dorsal view on segments 4–7; D: Ventral view on segments 4–7; E: Dorsal view on segments 8–11; F: Ventral view on segments 8–11. Abbreviations: dpl, dorsal placid; latu, lateral accessory tube; ltas, lateral terminal accessory spine; lts, lateral terminal spine; lvs, tateroventral spine; lvtu, lateroventral tube; mds, middorsal spine; ne, mvpl, midventral placid; nephridiopore; pf, papillary flap; te, tergal extension; numbers after abbreviations indicate corresponding segment; glandular cell outlets type 1 are marked as continuous circles, and sensory spots as dashed circles.

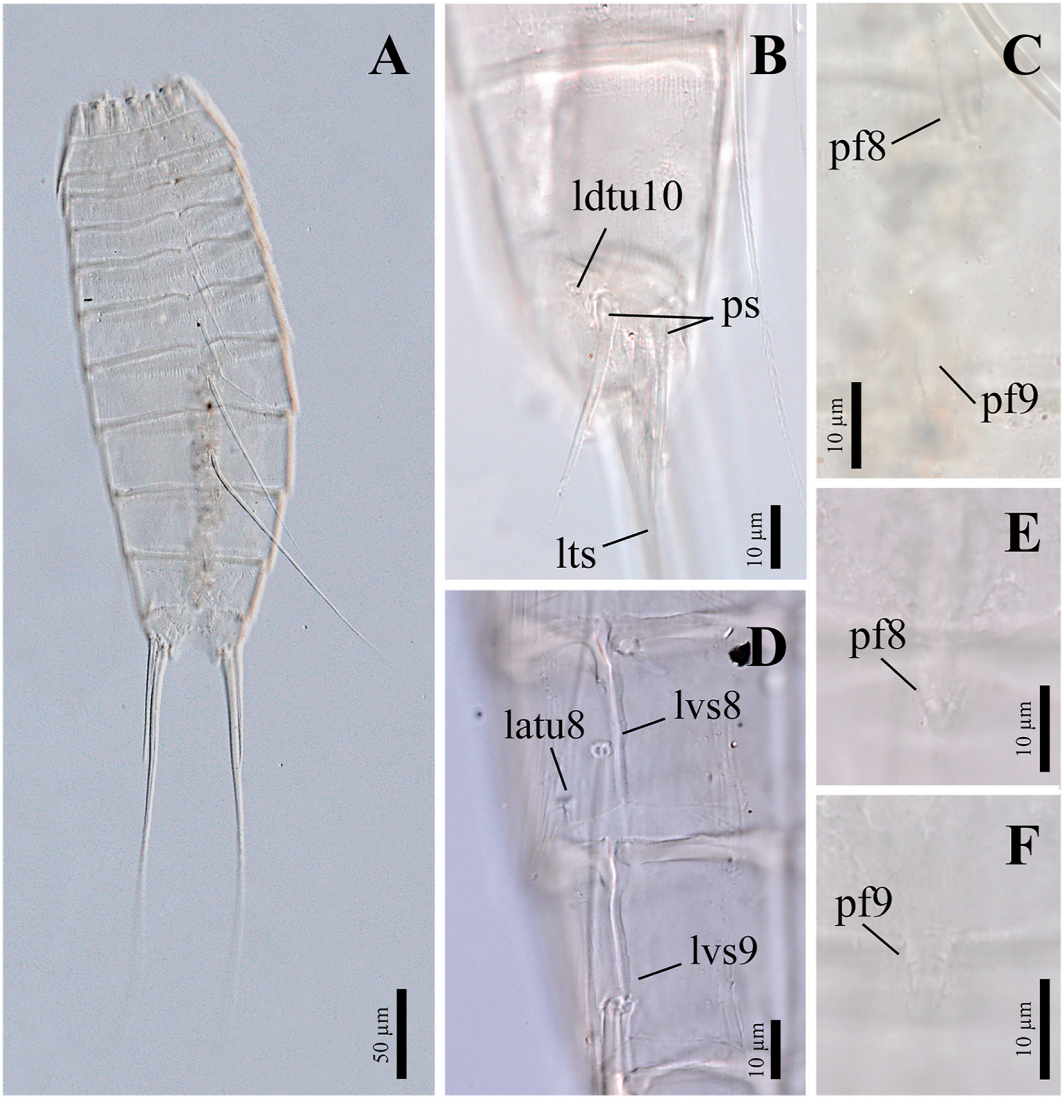

Fig. 4. Light micrographs of female holotype NHMD-1784619 (A, C), male paratype NHMD-1784622 (B), male paratype NHMD-1784623 (D) and male NHMD-1784620 of *Echinoderes australis* sp. nov., showing trunk overview and details on the segments 8–11. A: Dorsal trunk overview; B: Lateral view on right side of cuticular plates of segments 10–11; C: Close-up of papillary flap of segments 8 and 9; D: Ventral view on the right side on segments 8–9; E: Close-up of papillary flap of segment 8; F: Close-up of papillary flap of segment 9. Abbreviations: latu, lateral accessory tube; ldtu; laterodorsal tube; pf, papillary flap; ps; penile spine; lts, lateral terminal spine; lvs, tateroventral spine; numbers after abbreviations indicate corresponding segment.

3.1.4. Etymology

The species name, *australis*, derives from the Latin term "auster" (south) plus the suffix "-alis" (relation or belonging), referring to the area where the species was found, in the Southern Ocean.

3.1.5. Description

All dimensions and measurements are summarized in Table 1, and distribution of cuticular structures in Table 2.

None of the examined specimens had the head everted, hence no details on mouth cone and introvert can be provided.

Neck with 16 placids (Fig. 2 A–B, 3 A–B, 5 A–B). Midventral placid broadest (15-17 µm in width, 16-19 µm in length). Remaining placids similar in size and narrower than the midventral one (7-9 µm in width and 17-19 µm in length). Four dorsal and two ventral trichoscalid plates are present (Fig. 2A and B), each carrying a thick and feathery trichoscalid.

Trunk with 11 segments, with segments 1 and 2 as closed cuticular rings and the remaining segments formed by one tergal and two sternal plates (Fig. 2 A and B). Sternal plates reach their maximum width at segment 8, progressively tapering towards the last trunk segments, giving a slender appearance to the body. Cuticular hairs long, filiform, bracteate (Fig. 5 C), arranged in several wavy, transverse rows that extend from the paradorsal regions to the sternal plates (Fig. 2 A and B), except on segment 10 (devoid of hairs in middorsal and subdorsal regions) and 11 (almost completely devoid of hairs) (Fig. 2 A–D). Hairs well-spaced through the surface of each segment, uniformly distributed, except in middorsal, laterodorsal and ventromedial regions, forming hairless longitudinal bands (Fig. 2 A and B). Segments 1 to 5 with up to three dorsal rows of hairs, segments 6 to 10 with up to five dorsal rows of hairs; ventral side with three rows of hairs. Hairs of each anterior row surpass the insertion of the following one, and with those of the last row reaching the pectinate fringe of the segment. Sensory spots small, with a round to oval shape, composed of a single pore surrounded by few, short micropapillae (Fig. 5 F). Sensory spots of segment 1 larger, formed by a higher number of short micropapillae. Posterior segment margin straight, forming well-developed primary pectinate fringes with elongated, strongly serrated tips alternating in size (Fig. 5 B–C, E). Primary pectinate fringes of segments 7 to 10 reduce in size towards the middorsal region (Fig. 2 A–C). Secondary pectinate fringe well-developed, with short and thin serrated tips. Type 1 glandular cell

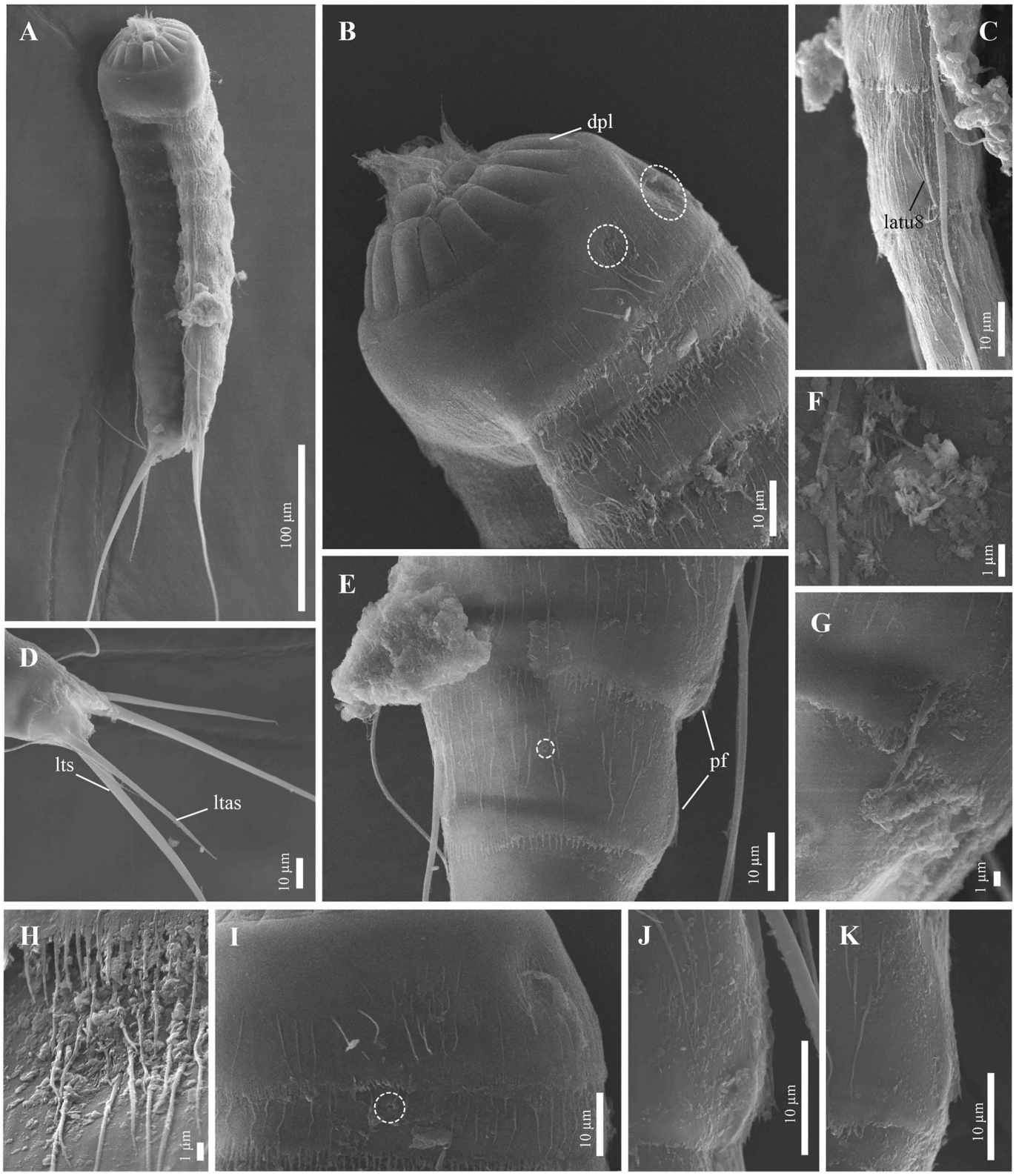

Fig. 5. Scanning electron micrographs of two female additional specimens (A62C 2-3) (A–B, D–G) (A62C 1-2) (C) of *Echinoderes australis* sp. nov. Showing trunk overview and cuticular details of the neck and trunk segments. A: Lateroventral trunk overview; B: Lateral view of the neck and segments 1–4; C: Detail of lateral accessory tube and lateroventral spine of segment 8; D: Detail of lateral terminal accessory and lateral terminal spines; E: Lateral view of segments 8–9, marking the papillary flaps; F: Detail of the ventromedial sensory spot on the right sternal plate of segment 7; G: Detail of the laterodorsal tube on the left side of segment 10; H: Detail of the midlateral sensory spot of segment 5; I: Lateral view of segments 1–2; J: Detail of the papillary flap of segment 8; K: Detail of the papillary flap of segment 9. Abbreviations: dpl, dorsal placid; latu, lateral accessory tube; ltas, lateral terminal accessory spine; lts, lateral terminal spine; lvs, lateroventral spine; pf, papillary flap; numbers after abbreviations indicate corresponding segment; sensory spots are marked as dashed circles.

Table 1
Measurements (μm) and proportions (%) of *Echinoderes australis* sp. nov. Numbers in the first column indicate the corresponding segment. Abbreviations: CL, cumulative length; LATu, lateral accessory tube; LDTu, laterodorsal tube; LTAS, lateral terminal accessory spine; LTS, lateral terminal spine; LVS, lateroventral spine; LVTu, lateroventral tube; MDS, middorsal spine; MSW, maximum sternal width, measured on segment 8; n, number of measured specimens; S, segment length; SD, standard deviation; SW, standard width, measured on segment 10; TL, total trunk length.

Character	Holotype	N	Mean♂	Range♂	Mean♀	Range♀	Mean♂♀	Range ♂♀	SD ♂♀
TL	305	2♂/1♀	311	309–313	305	–	309	305–313	4.0
CL	457	2♂/1♀	427	417–436	457	–	437	417–457	20.0
CL/TL	150 %	2♂/1♀	137 %	135–139	150 %	–	141 %	135 %–150 %	7.6
MSW 8	70	2♂/1♀	65	60–69	70	–	66	60–70	5.5
MSW/TL	23 %	2♂/1♀	21 %	19 %–22 %	23 %	–	22 %	19 %–23 %	1.8
SW10	61	2♂/1♀	56	54–58	61	–	58	54–61	3.5
S1	35	2♂/1♀	33	31–35	35	–	34	31–35	2.3
S2	33	2♂/1♀	27	27	33	–	29	27–33	3.5
S3	36	2♂/1♀	31	31	36	–	33	31–36	2.9
S4	40	2♂/1♀	35	34–36	40	–	37	34–40	3.1
S5	41	2♂/1♀	40	37–42	41	–	40	37–42	2.6
S6	47	2♂/1♀	42	40–44	47	–	44	40–47	3.5
S7	50	2♂/1♀	45	42–48	50	–	47	42–50	4.2
S8	51	2♂/1♀	49	48–49	51	–	49	48–51	1.5
S9	51	2♂/1♀	47	46–48	51	–	48	46–51	2.5
S10	39	2♂/1♀	48	46–50	39	–	45	39–50	5.6
S11	34	2♂/1♀	31	28–33	34	–	32	28–34	3.2
MDS4	46	1♂/2♀	41	–	45	43–46	43	41–46	2.5
MDS5	57	3♂/2♀	62	56–69	59	57–61	61	56–69	5.1
MDS6	67	3♂/2♀	75	71–78	68	67–69	72	67–78	4.7
MDS7	114	1♂/2♀	123	–	118	114–122	120	114–123	4.9
MDS8	176	2♂/2♀	187	186–187	185	176–194	186	176–194	7.4
LVTu5	14	1♂/2♀	9	–	15	14–16	13	9–16	3.6
LVS6	43	3♂/2♀	50	44–57	46	43–48	48	43–57	5.5
LVS7	59	3♂/2♀	58	50–67	59	59	59	50–67	6.0
LVS8	71	3♂/2♀	77	75–82	73	71–74	75	71–82	4.0
LATu8	16	1♂/2♀	10	–	13	10–16	12	10–16	3.5
LVS9	98	3♂/2♀	115	95–141	95	91–98	107	91–141	20.3
LDTu10	–	1♀	–	–	8	–	8	–	–
LTS	321	3♂/1♀	317	307–328	321	–	318	307–328	8.8
LTAS	74	2♀	–	–	79	74–84	79	74–84	7.1
LTS/TL	105 %	2♂/1♀	102 %	98 %–106 %	105 %	–	103 %	98 %–106 %	4.4
LTAS/TL	24 %	1♀	–	–	24 %	–	24 %	–	–
LTAS/LTS	23 %	1♀	–	–	23 %	–	23 %	–	–

Table 2
Summary of nature and arrangement of acicular spines, tubes, sensory spots, glandular cell outlets and nephridiopore in adults of *Echinoderes australis* sp. nov. Abbreviations: ac, acicular spine; f, female condition of sexually dimorphic character; gco1, type 1 glandular cell outlet; LA, lateral accessory; LD, laterodorsal; ltas, lateral terminal accessory spines; lts, lateral terminal spines; LV, lateroventral; m, male condition of sexually dimorphic character; MD, middorsal; ML, midlateral; PD, paradorsal; ps, penile spines; SD, subdorsal; ss, rounded sensory spot; tu, tube; VL, ventrolateral; VM, ventromedial.

Segment	MD	PD	SD	LD	ML	LA	LV	VL	VM
1	gco1, gco1		Ss	Ss			gco1		
2	gco1		Ss						gco1, ss
3	gco1								gco1
4	ac	gco1							gco1
5	ac	gco1			ss		tu		gco1
6	ac	gco1			ss		ac		gco1
7	ac	gco1					ac		gco1, ss
8	ac, pf	gco1, ss				tu	ac		gco1
9	pf	gco1, ss	Ss	Ss			ac	ss	gco1
10	gco1, gco1		ss	Tu				ss	gco1
11	gco1, gco1	ss	ss	ps(m)		ltas(f)	lts		

outlets are located at the anterior dorsal region of the segments, except the posterior outlets of segment 1, 10 and 11 that are located towards the middle region of the plate (Fig. 2 A–D).

Segment 1 without spines or tubes. Two type 1 glandular cell outlets in middorsal position, longitudinally aligned, and one pair in lateroventral position (Fig. 2 A–B, 3 A–B). Paired sensory spots in subdorsal and laterodorsal positions (Figs. 3 A and 5 B). Pectinate fringe less developed than on following segments (Fig. 5 B).

Segment 2 without spines or tubes. Unpaired middorsal type 1 glandular cell outlet and paired ones in ventromedial positions (Fig. 2 A–B, 3 A). Paired sensory spots in subdorsal and ventromedial positions (Fig. 2 A–B, 5 I).

Segment 3 without spines or tubes. Unpaired middorsal type 1 glandular cell outlet and paired ones in ventromedial position (Fig. 2 A–B, 3 A–B).

Segment 4 with a middorsal acicular spine, reaching the posterior margin of the following segment (Fig. 3 A–C). Paired paradorsal and ventromedial type 1 glandular cell outlets (Fig. 3 A–D).

Segment 5 with a middorsal acicular spine longer than of preceding segment, reaching the posterior margin of the following segment, and one pair of lateroventral tubes (Fig. 3 C and D). Paired paradorsal and ventromedial type 1 glandular cell outlets (Fig. 3 C and D). Paired midlateral sensory spots (Fig. 3 C–D, 5 H).

Segment 6 with a middorsal acicular spine longer than of preceding

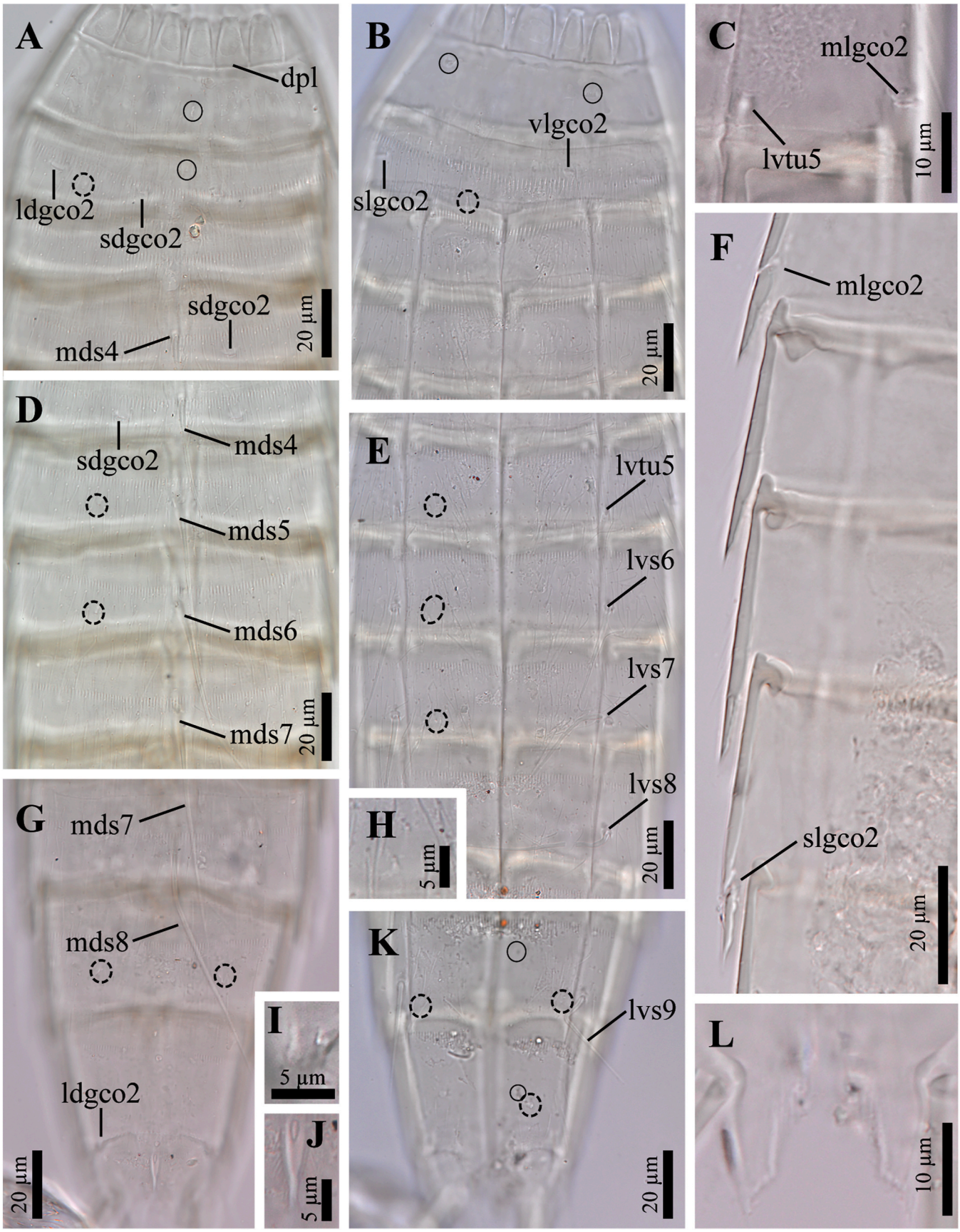

(caption on next page)

Fig. 6. Light micrographs of female of *Echinoderes* cf. *angustus* showing trunk overview and details on the segments 8–11. A: Dorsal view on the neck and segments 1–4; B: Ventral view on the neck and segments 1–4; C: Close-up of midlateral glandular cell outlet type 2 of segments 5; D: Dorsal view on segments 4–7; E: Ventral view on segments 5–8; F: Midlateral and sublateral glandular cell outlet type 2 on segments 5 and 8, respectively; G: Dorsal view on segments 8–11; H: Close-up of ventromedial sensory spot of segment 6; I: Close-up of laterodorsal glandular cell outlet type 2 of segment 10; J: Close-up of the pointed, middorsal protuberance of segment 11; K: Ventral view on segments 9–11; L: Close-up of tergal extensions. Abbreviations: dpl, dorsal placid; ldgco2, laterodorsal glandular cell outlet type 2; lvs, tateroventral spine; lvtu, lateroventral tube; mds, middorsal spine; mlgco2, midlateral glandular cell outlet type 2; sdgco2, subdorsal glandular cell outlet type 2; slgco2, sublateral glandular cell outlet type 2; vlgco2, ventrolateral glandular cell outlet type 2; numbers after abbreviations indicate corresponding segment; glandular cell outlets type 1 are marked as continuous circles, and sensory spots as dashed circles.

segment, reaching medially on segment 8 (Fig. 3 C); and one pair of lateroventral acicular spines, reaching the posterior margin of segment 7 (Fig. 3 D). Paired paradorsal and ventromedial type 1 glandular cell outlets (Fig. 3 C and D). Paired midlateral sensory spots (Fig. 3 C and D).

Segment 7 with a middorsal acicular spine longer than of preceding segment, reaching medially on segment 10 (Fig. 3 C–E); and one pair of lateroventral acicular spines longer than those of the preceding segment, reaching the posterior margin of segment 8 (Fig. 3 D–F). Paired paradorsal and ventromedial type 1 glandular cell outlets (Fig. 3 C and D). Paired sensory spots in ventromedial position (Figs. 2 B and 5 F). Primary pectinate fringe reduces in size towards the middorsal region (Fig. 2 A–C).

Segment 8 with a whip-like middorsal acicular spine much longer than on preceding segment, exceeding far beyond the posterior margin of segment 11 (Figs. 3 E and 4 A). One pair of lateroventral acicular spines longer than those of the preceding segment, reaching the medially on segment 10 (Figs. 3 F, 4 D and 5 C). One pair of long tubes in lateral accessory position (Figs. 3 F, 4 D and 5 C). Paired paradorsal and ventromedial type 1 glandular cell outlets (Fig. 3 E–F). A papillary middorsal flap located at the most posterior margin of the segment (Figs. 3 E, 4 C, E, 5 E, J), flanked by a pair of paradorsal sensory spots (Fig. 2 A). Primary pectinate fringe reduces in size towards the middorsal region (Fig. 2 A–C, 5 E).

Segment 9 with one pair of very long lateroventral acicular spines, exceeding well beyond the posterior margin of segment 11; the distal end is whip-like (Figs. 3 F, 4 D and 5 A). Paired paradorsal and ventromedial type 1 glandular cell outlets (Fig. 2 A–B, 3 F). Longer papillary middorsal flap than on preceding segment (Figs. 3 E, 4C, F, 5 E, K), located at the posterior margin of the segment, and flanked by a pair of paradorsal sensory spots (Fig. 2 A). Three additional pairs of sensory spots located in subdorsal, laterodorsal and ventrolateral positions (Fig. 3 E–F, 5 E). Subdorsal and laterodorsal pairs located in the middle of the segment; ventrolateral pair located near the posterior segment margin. Rounded nephridiopores as sieve plates in sublateral position (Fig. 3 F). Primary pectinate fringe reduces in size towards the middorsal region (Fig. 2 A–C).

Segment 10 with paired, long and slender laterodorsal tubes near posterior segment margin with similar appearance in both sexes (Fig. 2A–C, 4 B, 5 G). Two longitudinally arranged middorsal type 1 glandular cell outlets and paired ones in ventromedial position (Fig. 2 A–D). Pairs of sensory spots in subdorsal and ventrolateral positions (Fig. 2 A–D, 3 F). Subdorsal pair located in the middle of the segment; ventrolateral pair located near the posterior segment margin. Margins of the sternal plates midventral extended (Fig. 2 B–D, 3 F). Primary pectinate fringe reduces in size towards the middorsal region (Fig. 2 A–C).

Segment 11 with a pair of very long lateral terminal spines (Fig. 2 A–D, 3 E, 4 A–B, 5 D). Females with strong and stout pair of lateral terminal accessory spines (Fig. 2 A–B, 3 E, 4 A, 5 D). Males with three stout pairs of penile spines: the median ones stouter than the other two pairs (Fig. 4 B). Two longitudinally arranged middorsal type 1 glandular cell outlets (2 A and C). Sensory spots in paradorsal and subdorsal positions (Fig. 2 A–C). The paradorsal pair located posteriorly to the subdorsal ones. Pectinate fringe with short tips, except in lateral margins where are a bit longer. Tergal extensions short and triangular (Fig. 3 E) and with hairy mesial areas. The posterior margin of the sternal plates rounded, similar in length to the tergal extensions.

3.2. Other kinorhynch species

Echinoderes australis sp. nov. occurred with two additional species of *Echinoderes*: *Echinoderes* cf. *angustus* Higgins and Kristensen, 1988 (one specimen); and a species with a combination of characters that made exact identification uncertain, *Echinoderes* sp. 1 (two specimens). *Echinoderes* cf. *angustus* and *Echinoderes* sp. 1 occurred with the new species in station A5200; whereas *E. australis* sp. nov. was the single species found in station A6200.

Echinoderes cf. *angustus* (Fig. 6 and Table 3)

Material examined: female, collected in 2019/12/19 at South Orkney Trench, Southern Ocean: Station A5200; Coordinates 60° 52′ 30.000″ S, 41° 36′ 2.400″ W; at 5.251 m depth; mounted in DMHF, deposited at NHMD under catalogue number: NHMD-XXXX.

Table 3
Measurements (μm) and proportions (%) of *Echinoderes* cf. *angustus*. Numbers in the first column indicate the corresponding segment. Abbreviations: CL, cumulative length; LTAS, lateral terminal accessory spine; LTS, lateral terminal spine; LVS, lateroventral spine; MDS, middorsal spine; MSW, maximum sternal width, measured on segment 6; S, segment length; SW, standard width, measured on segment 10; TL, total trunk length.

Character	♀ *Echinoderes* cf. *Angustus*
TL	316
CL	465
CL/TL	147 %
MSW 6	55
MSW/TL	17 %
SW10	46
S1	36
S2	33
S3	38
S4	40
S5	43
S6	46
S7	51
S8	54
S9	51
S10	45
S11	28
MDS4	52
MDS5	63
MDS6	68
MDS7	77
MDS8	92
LVTu5	–
LVS6	38
LVS7	39
LVS8	42
LVS9	36
LTS	223
LTAS	51
LTS/TL	71 %
LTAS/TL	16 %
LTAS/LTS	23 %

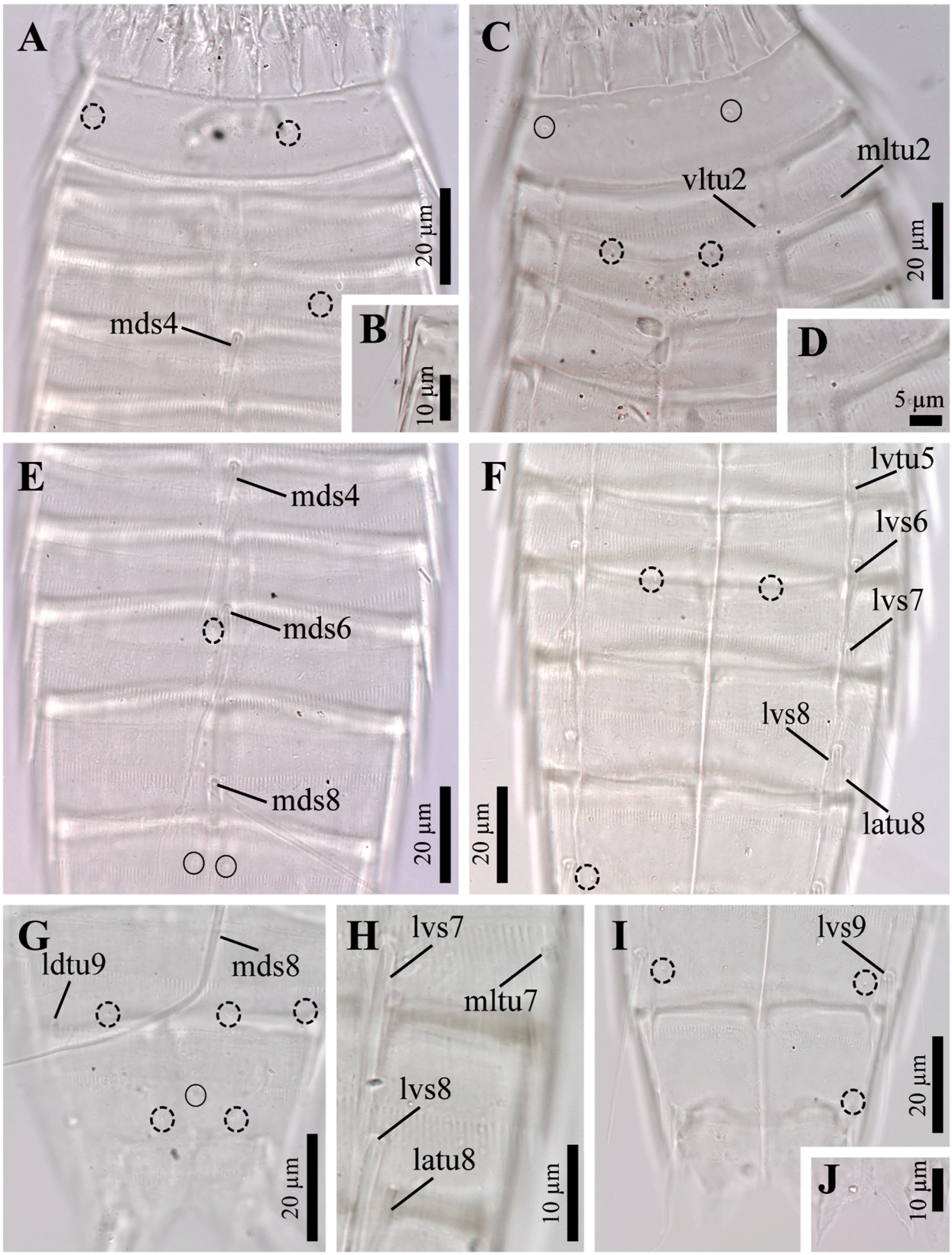

Fig. 7. Light micrographs of males of *Echinoderes* sp. 1 showing trunk overview and details on the segments 8–11. A: Dorsal view on the neck and segments 1–5; B: Close-up of midlateral tube of segment 2; C: Ventral view on the neck and segments 1–4; D: Close-up of ventrolateral and midlateral tubes of segment 2; E: Dorsal view on segments 5–8; F: Ventral view on segments 5–9; G: Dorsal view on segments 9–11; H: Lateral view on segments 7–8; I: Ventral view on segments 9–11; J: Close-up of tergal extensions. Abbreviations: latu, lateral accessory tube; ldtu, laterodorsal tube; lvs, tateroventral spine; lvtu, lateroventral tube; mds, middorsal spine; mltu, midlateral tube; vltu, ventrolateral tube; numbers after abbreviations indicate corresponding segment; glandular cell outlets type 1 are marked as continuous circles, and sensory spots as dashed circles.

Table 4
Measurements (μm) and proportions (%) of *Echinoderes* sp. 1. Numbers in the first column indicate the corresponding segment. Abbreviations: CL, cumulative length; LATu, lateral accessory tube; LDTu, laterodorsal tube; LTS, lateral terminal spine; LVS, lateroventral spine; LVTu, lateroventral tube; MDS, middorsal spine; MLTu, midlateral tube; MSW, maximum sternal width, measured on segment 6; S, segment length; SW, standard width, measured on segment 10; TL, total trunk length; VLTu, ventrolateral tube.

Character	♂ *Echinoderes* sp. 1	♂ *Echinoderes* sp. 1
TL	201	214
CL	352	351
CL/TL	175 %	164 %
MSW 6	54	57
MSW/TL	27 %	27 %
SW10	46	46
S1	28	29
S2	24	25
S3	25	25
S4	29	29
S5	32	31
S6	35	34
S7	37	37
S8	39	39
S9	40	42
S10	36	35
S11	27	25
MDS4	–	34
MDS6	54	–
MDS8	86	84
MLTu2	–	16
VLTu2	–	–
LVTu5	–	–
LVS6	25	29
LVS7	35	34
LVS8	44	40
LATu8	–	–
LVS9	41	42
LDTu9	–	–
LDTu10	–	–
LTS	–	151
LTS/TL	–	71 %

3.2.1. *Brief description*

Echinoderes with middorsal spines present on segments 4 to 8, and spines in lateroventral positions on segments 6 to 9. Tubes in lateroventral positions on segment 5. Glandular cell outlets type 2 in subdorsal, laterodorsal, sublateral and ventrolateral positions on segment 2, subdorsals on segment 4, midlateral on segment 5,sublateral on segment 8 and laterodorsal on segment 10.

Adults with head, neck and eleven segments. Overview of measures and dimensions are given in Table 3.

Segments 1 and 2 as complete cuticular rings (Fig. 6 A and B). Segment 1 with a single middorsal glandular cell outlet type 1 and a pair in lateroventral positions (Fig. 6 A and B), plus subdorsal sensory spots. Segment 2 with subdorsal, laterodorsal, sublateral and ventrolateral glandular cell outlets type 2, plus a single middorsal glandular cell outlet type 1 and a pair in ventromedial positions, and subdorsal and ventromedial sensory spots (likely also in midlateral positions) (Fig. 6 A and B). Segment 3 without any conspicuous cuticular structures (Fig. 6 A and B), except for a single middorsal glandular cell outlet type 1, a pair in ventromedial positions, plus subdorsal sensory spots (likely also in sublateral positions). Segment 4 with acicular middorsal spine, subdorsal glandular cell outlets type 2 (Fig. 6 A–D), plus paradorsal and ventromedial glandular cell outlets types 1, present on this and following five segments. Segment 5 with acicular middorsal spine and lateroventral tubes, midlateral glandular cell outlets type 2, and subdorsal and ventromedial sensory spots (Fig. 6 C–F). Segment 6 with acicular middorsal and lateroventral spines, plus subdorsal and ventromedial sensory spots (likely also in paradorsal and midlateral positions) (Fig. 6 D–E, H). Segment 7 with acicular middorsal and lateroventral spines, and ventromedial sensory spots (likely also in paradorsal and midlateral positions) (Fig. 6 D–E, G). Segment 8 with acicular middorsal and lateroventral spines, plus sublateral glandular cell outlets type 2 (Fig. 6 E–G), and paradorsal sensory spots. Segment 9 with lateroventral spines, and sensory spots in paradorsal, subdorsal and ventrolateral positions (likely also in midlateral positions) (Fig. 6 G–K). Rounded, small sieve plates in sublateral positions. Segment 10 with laterodorsal structure, likely glandular cell outlets type 2 (Fig. 6 G–I), single middorsal glandular cell outlet type 1 and a pair in ventromedial positions, plus laterodorsal and ventromedial sensory spots (Fig. 6 G–K). Posterior edge of segments 1 to 10 with primary pectinate fringe. Segment 11 with long lateral terminal spines, thin lateral terminal accessory spines, sensory spots in subdorsal positions and two glandular cell outlets type 1 located middorsal. Conspicuous protuberance, pointed forward in middorsal position (Fig. 6 J). Tergal extensions short and triangular (Fig. 6 L). The posterior margins of the sternal plates rounded, shorter than tergal extensions.

Echinoderes sp. 1 (Fig. 7 and Table 4)

Material examined: two males, collected in 2019/12/19 at South Orkney Trench, Southern Ocean: Station A5200; Coordinates 60° 52′ 30.000″ S, 41° 36′ 2.400″ W; at 5.251 m depth; mounted in DMHF, deposited at NHMD under catalogue number: NHMD-XXXX and NHMD-XXXX.

3.2.2. *Brief description*

Echinoderes with middorsal spines present on segments 4, 6 and 8, and spines in lateroventral positions on segments 6 to 9. Tubes in midlateral and ventrolateral positions on segment 2, lateroventral ones on segment 5, lateral accessory on segment 8, and laterodorsal on segments 9 and 10. Midlateral tubes on segment 7 to be confirmed.

Adults with head, neck and eleven segments. Overview of measures and dimensions are given in Table 4.

Segments 1 and 2 as complete cuticular rings (Fig. 7 A–C). Segment 1 with a single middorsal glandular cell outlet type 1 and a pair in lateroventral positions, sensory spots in subdorsal and laterodorsal positions (Fig. 7 A–C). Sensory spots on this and following segments are very small, visible as a single dot or two dots in LM observations. Segment 2 with midlateral and ventrolateral tubes (Fig. 7 B–D), a single middorsal and a pair of ventromedial glandular cell outlets type 1, plus ventromedial sensory spots (Fig. 7 C). Segment 3 with subdorsal sensory spots (Fig. 7 A), a single middorsal glandular cell outlet type 1 and a pair in ventromedial positions. Segment 4 with acicular middorsal spine (Fig. 7 A–E), paradorsal and ventromedial glandular cell outlets types 1, present on this and following six segments. Segment 5 with lateroventral tubes (Fig. 7 F). Segment 6 with acicular middorsal and lateroventral spines, plus sensory spots in paradorsal and ventromedial positions (Fig. 7 E–F). Segment 7 with lateroventral spines (Fig. 7 F–H), and likely midlateral tubes in one specimen (Fig. 7 H). Segment 8 with acicular middorsal and lateroventral spines, lateral accessory tubes (Fig. 7 E–H), and paradorsal sensory spots. Segment 9 with lateroventral spines, laterodorsal tubes, and sensory spots in subdorsal, laterodorsal and ventrolateral positions (Fig. 7 E–G, I). Rounded, small sieve plates in lateral accessory positions. Segment 10 with laterodorsal tubes, two middorsal glandular cell outlet type 1 and a pair in ventromedial positions, plus sensory spots in subdorsal and ventrolateral positions (Fig. 7 G–I). Posterior edge of segments 1 to 10 with primary pectinate fringe. Segment 11 with long lateral terminal spines, three pairs of penile spines, sensory spots in subdorsal positions and two glandular cell outlets type 1 located middorsal. Tergal extensions short and pointed (Fig. 7 J). The posterior margins of the sternal plates rounded, shorter than tergal extensions.

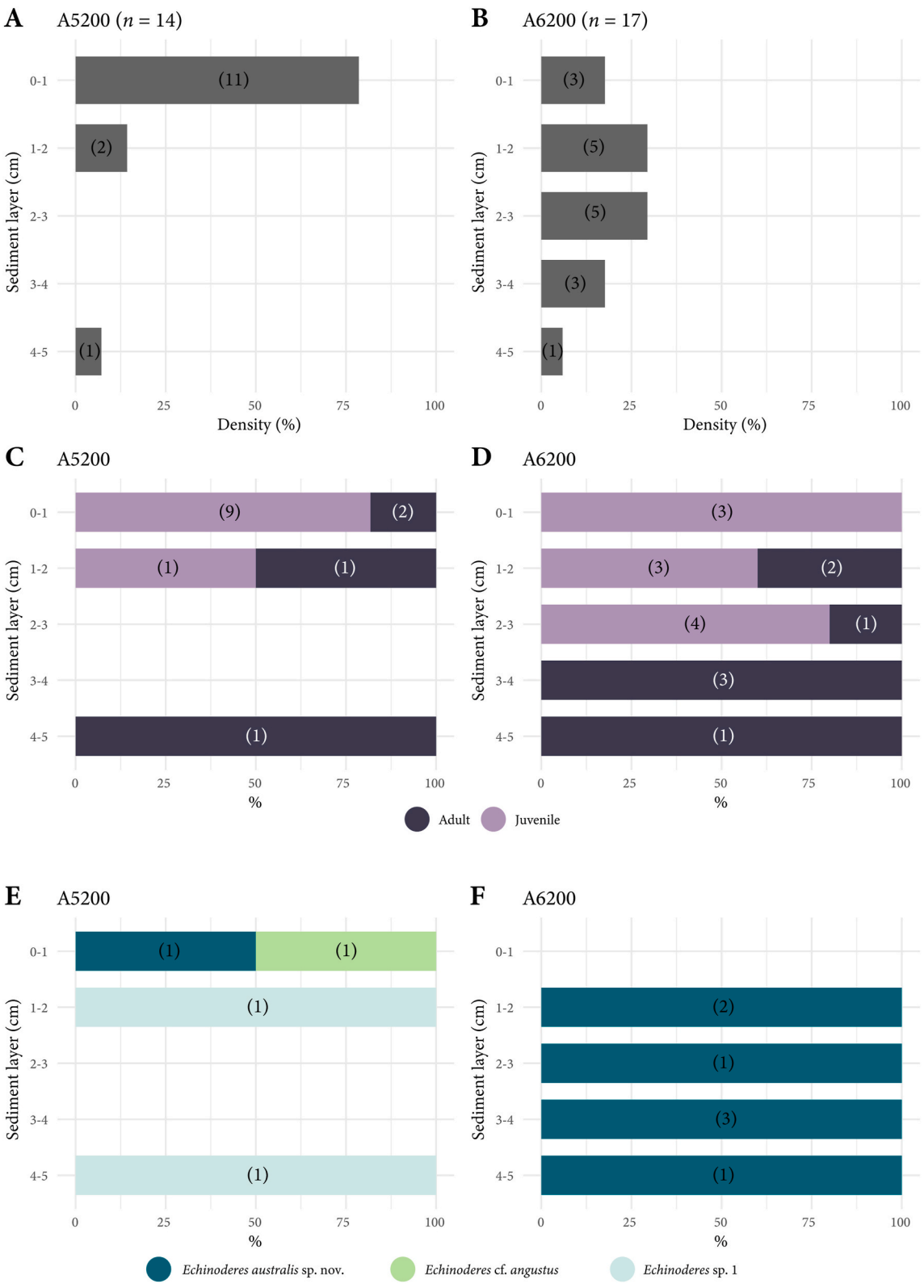

Fig. 8. A–B: Total percentage of kinorhynchs along the vertical profile of the two study sites, A5200 and A6200. C–D: Adult (deep purple) and juvenile (light purple) density along the vertical profile of the two study sites, A5200 and A6200. E–F: Species percentage along the vertical profile of the two study sites, A5200 and A6200; *Echinoderes* cf. *angustus* (olive green), *Echinoderes australis* sp. nov (aquamarine green), *Echinoderes* sp.1 (light green). Numbers in brackets indicate the number of specimens collected at each layer.

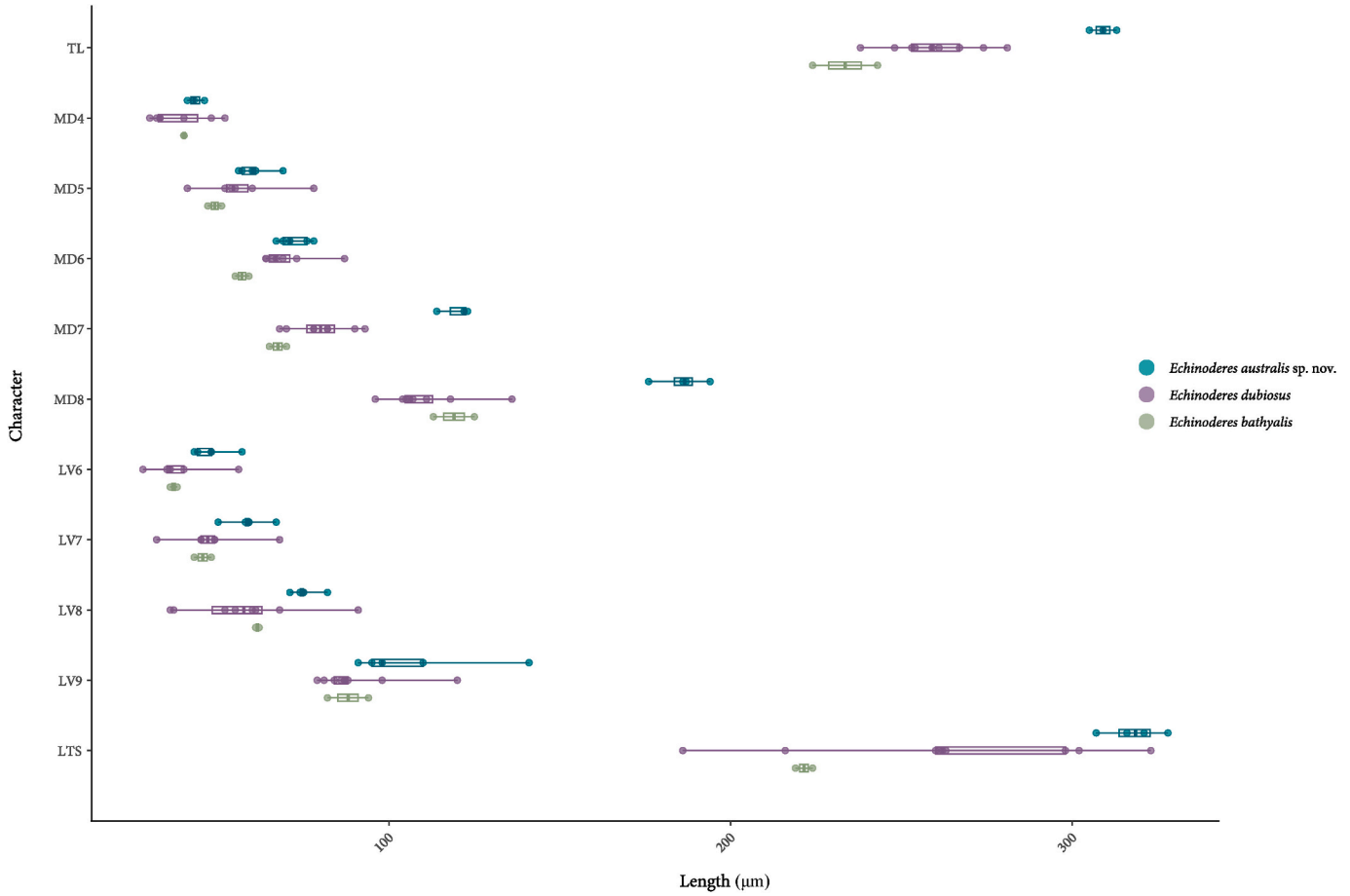

Fig. 9. Variation in length of selected measurements of *Echinoderes australis* sp. nov (aquamarine green), *Echinoderes dubiosus* (purple) and *Echinoderes bathyalis* (olive green). Points mark the values and boxplots mark the median value (horizontal line within the box). Abbreviations: LTS, lateral terminal spine; LV, lateroventral spine; MD, middorsal spine; TL, total trunk length; numbers after abbreviations indicate corresponding segment.

3.3. Kinorhyncha distribution

The kinorhynch community showed a different arrangement between the axis (station A6200) and the terrace (station A5200) (Fig. 8). At the terrace, kinorhynchs were concentrated in the top 1 cm layer of sediment, whereas axis specimens were distributed more homogeneously through the vertical profile, being present in all five depth intervals of 1 cm each. Similar number of specimens, with high a proportion of juvenile stages, were present at both studied sites: 14 specimens at A5200 (71 % juveniles, 29 % adults), and 17 specimens at A6200 (59 % juveniles, 41 % adults). All adult specimens from A6200 belonged to the new species. At both stations, juvenile stages appeared only in the upper depth horizons (Fig. 8): in layers 0-1 and 1-2 at station A5200; and in layers 0-1, 1-2, and 2-3 at station A6200.

4. Discussion

4.1. Taxonomic remarks of Echinoderes australis sp. nov

E. australis sp. nov. has middorsal spines on segments 4-8 and lateroventral spines on segments 6-9, which is the most common spine pattern among the genus *Echinoderes* (Yamasaki et al., 2020).

However, the absence of additional cuticular structures (spines, tubes or type 2 glandular cell outlets) on segment 2 is in fact an unusual condition, shared by only two species with the same spine formula, namely *Echinoderes kaempfae* Yamasaki et al., 2019 and *Echinoderes pterus* Yamasaki et al., 2018a. Nevertheless, *E. australis* sp. nov. is very easily distinguishable from these two species, as they both lack the lateral accessory tube on segment 8, present in the new species. Furthermore, *E. kaempfae* is distinguished by its very characteristic long and pointy tergal extensions while *E. pterus* has tufts of long hairs arising from slits on segment 9 (Yamasaki et al., 2018a, 2019), both features absent in *E. australis* sp. nov.

Among the echinoderms inhabiting the deep ocean, the new species shows many similarities with *Echinoderes bathyalis* Yamasaki et al., 2018b, *Echinoderes dubiosus* Sørensen et al., 2018 and *E. mamaqucha*. The four species have an identical spine pattern and lateroventral tubes on segment 5 (Sørensen et al., 2018; Yamasaki et al., 2018b; Grzelak et al., 2021). *Echinoderes mamaqucha* shares with *E. australis* sp. nov. the presence of lateral accessory tubes on segment 8 and middorsal papillary flaps on segments 8 and 9, but it is the easiest to differentiate from the new species since it has dorsal and ventral tubes on segment 2 (Grzelak et al., 2021), a character absent in the species from the South Orkney Trench. It is more complicated to differentiate *E. australis* sp. nov. from *E. bathyalis* and *E. dubiosus*, being even difficult to differentiate between the latter two. In fact, in the original description of *E. dubiosus*, the similarity of this species to *E. bathyalis* was already discussed in detail, and is even reflected in the naming of the species itself. The main difference between the two species is the presence of the lateral tube in segment 8 in *E. dubiosus*, absent in *E. bathyalis*, and the slight difference in length of the lateroventral spine of segment 9, which is longer in *E. dubiosus* (Sørensen et al., 2018). Moreover, there are some differences in the pattern of sensory spots, and *E. dubious* possesses a papillary flap on segment 9, a feature absent in *E. bathyalis*.

Likewise, *Echinoderes australis* sp. nov. is also very close to both species, with long spines and with the lateroventral spines of segment 9

extending well beyond segment 11. Especially the new species closely resembles *E. dubious* since, in addition to the similarities with the other congeners mentioned, it has a lateral tube on segment 8 and a papillary flap on segment 9. However, the new species also has a very conspicuous papillary flap on segment 8, posterior to the spine, which is absent in *E. dubiosus*. More importantly, *E. australis* sp. nov. lacks completely type 2 glandular cell outlets in segment 2, a character that both *E. bathyalis* and *E. dubiosus* possess. The lengths of the spines on the posterior segments, both the middorsal and lateroventral ones, are also remarkable greater compared to those of *E. dubiosus* and *E. bathyalis* (Fig. 9): the average spine length/total length of the middorsal spine of segment 8 is $>$ 60 % in *E. australis* sp. nov., whereas the average spine length/total length is $<$43 % in *E. dubiosus*.

There are also differences in the pattern of sensory spots. Although these structures are not usually used to differentiate species completely, they have been used for this purpose together with other minor taxonomic differences such as length ratios or type 1 glandular cell outlets. Thus, *E. australis* sp. nov. has a different pattern of sensory spots than *E. bathyalis* and *E. dubiosus*, especially on the anterior segments. In addition, the new species has laterodorsal sensory spots on segments 5 and 6, whereas *E. bathyalis* lacks sensory spots on those segments in any lateral position, and *E. dubiosus* has only sensory spots on segment 5 but in a sublateral position.

Furthermore, the three species are from deep-sea, but are very far apart from a biogeographical viewpoint: *Echinoderes bathyalis* was described from the Northeast Atlantic, at the Sedlo Seamount; *E. dubiosus* was described from the North Pacific Ocean, in the US West Coast; and the new species is described from the Southern Ocean, in the South Orkney Trench. The extreme geographical distance between these morphologically similar species does not automatically accept them as different species (cosmopolitan and widely distributed species are known in this animal group; Neuhaus and Sørensen, 2013; Sánchez et al., 2022), but it is an incentive to accept small morphological differences as potentially distinguishing between them.

There is another hadal *Echinoderes* species not formally described, *Echinoderes* sp. 2, reported from the Atacama Trench (Grzelak et al., 2021). In the referred publication, the authors assumed *Echinoderes* sp. 2 represents a new species but did not describe it because the information was based in the examination of a single specimen. Instead of a formal description, they provided the most relevant morphological characters of the specimen, which perfectly fits with the morphometrics and cuticular structures present in *E. australis* sp. nov. Both species share spine, tube, glandular cell outlet type 1 and type 2 pattern as well as middorsal papillary flaps on segments 8 and 9. The only difference is the presence of a few sensory spots in *E. australis* sp. nov. that are absent in *Echinoderes* sp. 2. A reexamination of the single available specimen of *Echinoderes* sp. 2 allowed to identify midlateral structures on segment 5 that can represent sensory spots. Additionally, the presence of laterodorsal sensory spots of segment 9 was also confirmed and the paradorsal pair reported by Grzelak et al. (2021) can be the subdorsal pair described in *E. australis* sp. nov. Therefore, based on all abovementioned similarities, we suggest that the singleton found at the Atacama Trench and reported as *Echinoderes* sp. 2 in Grzelak et al. (2021) is identical with *E. australis* sp. nov.

4.2. Taxonomic remarks of Echinoderes cf. angustus

The spine, tube, glandular cell outlet type 1 and 2 pattern of the specimen found in the South Orkney Trench matches that of *Echinoderes angustus* (Higgins and Kristensen, 1988). Both species have spines in middorsal positions on segments 4 to 8 and in lateroventral positions on segments 6 to 9, tubes in lateroventral positions on segment 5, glandular cell outlets type 2 in subdorsal, laterodorsal, sublateral and ventrolateral positions on segment 2, subdorsal on segment 4, midlateral on segment 5, sublateral on segment 8 and laterodorsal on segment 10 (this latter structure was described as uncertain in Grzelak and Sørensen, 2018). In addition, the trunk dimensions of the South Orkney Trench specimen fall within the female size ranges reported in the original description of *E. angustus* (Higgins and Kristensen, 1988). However, the re-examination of type material of *E. angustus* showed a TL of 405 μm (Grzelak et al., 2023) and, therefore, larger dimensions than that of the new species. The spine lengths of the South Orkney Trench specimen do fit within the female size ranges reported of *E. angustus* (Higgins and Kristensen, 1988), except for the lateral terminal spines (see Table 3). According to the description, females of *E. angustus* have lateral terminal spines between 140 and 180 μm in length, whereas the size of these spines in the female of the South Orkney Trench reaches 223 μm. Based on this remarkable c. a. 25 % difference in the length of the lateral terminal spines, together with the presence of a conspicuous middorsal structure of segment 11 in the South Orkney Trench specimen, the absence of the characteristic midventral thickening of segment 2 of *E. angustus*, and the geographical distance between both species (*E. angustus* has been reported only from the Arctic region), the authors prefer to be cautious and identify the South Orkney Trench specimen as *E.* cf. *angustus*.

4.3. Taxonomic remarks of Echinoderes sp. 1

The presence of laterodorsal tubes on segment 9 is a rare character within the genus, reported for only nine species: *Echinoderes belenae* Pardos et al., 2016; *Echinoderes daenerysae* Grzelak and Sørensen, 2018; *Echinoderes dalzottoi* Grzelak and Sørensen, 2022; *Echinoderes frodoi* Grzelak and Sørensen, 2022; *Echinoderes gandalfi* Grzelak and Sørensen, 2022; *Echinoderes hviidarum* Sørensen et al., 2018; *Echinoderes leduci* Grzelak and Sørensen, 2022; *E. ultraabyssalis* and in an undescribed species from the Atacama Trench, named *Echinoderes* sp. 1 and hereafter referred to as the undescribed Atacama Trench species to avoid misunderstandings with the *Echinoderes* sp. 1 from the South Orkney Trench (Pardos et al., 2016; Grzelak and Sørensen, 2018; Sørensen et al., 2018; Adrianov and Maiorova, 2019; Grzelak et al., 2021, 2022). Of them, *E. daenerysae*, *E. dalzottoi*, *E. gandalfi*, *E. hviidarum*, *E. ultraabyssalis* and the undescribed Atacama Trench species have only two middorsal spines, on segments 6 and 8 (Grzelak and Sørensen, 2018; Adrianov and Maiorova, 2019; Grzelak et al., 2021); whereas *Echinoderes* sp. 1 has three middorsal spines, on segments 4, 6 and 8. Only three of the abovementioned species, *E. belenae*, *E. frodoi* and *E. leduci*, have middorsal spines on segments 4, 6 and 8, tubes in sublateral/lateral accessory positions on segment 8, in laterodorsal positions on segment 9 and in laterodorsal positions on segment 10 (the latter at least in males) (Pardos et al., 2016; Grzelak and Sørensen, 2022). *E. belenae* is easily distinguished from *Echinoderes* sp. 1 by very short lateral terminal spines and a high number of tubes, bearing at least thirteen pairs along the body (Pardos et al., 2016). The discrimination from *E. frodoi* and *E. leduci* is more complicated as all three have a very similar general appearance and morphometrics, and proper identification is based primarily on the number and position of tubes on segment 2. Observation of these tubes can be difficult as their identification depend on the degree of overlap between adjacent segments, as well as the preservation and mounting of specimens. *E. frodoi* has four pairs of tubes on segment 2, in subdorsal, laterodorsal, sublateral and ventrolateral positions (Grzelak and Sørensen, 2022); and *E. leduci* has two pairs of tubes on segment 2, in laterodorsal and ventrolateral positions (Grzelak and Sørensen, 2022). Thus, *E. leduci* fits with *Echinoderes* sp. 1 in the pattern of spines and tubes (pending confirmation of the presence/absence of the tube on segment 7 in *Echinoderes* sp. 1, which is absent in *E. leduci*), Moreover, both species have similar morphometrics (see Table 4), but show important differences in the arrangement of the sensory spots and in the type of cuticular hairs and perforation sites.

At this point we cannot forget that our statements about *Echinoderes* sp. 1 come from the observation of only two specimens. Taking this into account as well as the fact that minute sensory spots (like those of the species under study) and tubes can be difficult to identify (mainly those of segment 2), the morphological differences of *Echinoderes* sp. 1 with

E. frodoi and *E. leduci* can be due to an inaccurate observation of the structures in the South Orkney Trench specimens. Therefore, the authors prefer to leave the species as *Echinoderes* sp. 1, rather than assigning it to a previously described species or assuming that it represents a new species.

4.4. Diversity patterns and distribution of Kinorhyncha in the South Orkney Trench

It is known that meiofaunal density is inversely proportional to the seafloor depth. However, several studies carried out in hadal trenches have revealed that the abundance pattern changes in these environments, so higher densities than expected are found at depths of 6.000 m (Danovaro et al., 2002; Jamieson et al., 2010; Schmidt and Martínez Arbizu, 2015; Leduc et al., 2016). Within trenches the density of organisms shows a heterogeneous pattern, reaching higher values in the axis than in the terrace or slopes. This fact is due to axis acts as a reservoir of organic matter falling from the surface, allowing high microbial activity (Wenzhöfer et al., 2016; Glud et al., 2021; Xu et al., 2021) that supports meiofaunal communities (Danovaro et al., 2003; Glud et al., 2013; Shimabukuro et al., 2022).

Although in our investigation on kinorhynchs of the South Orkney Trench we studied only two sampling stations, one abyssal on the slope and one hadal on the axis, the results agree with those found in the Atacama Trench by Grzelak et al. (2021). If we attend only to the number of adults, there is a clear tendency of increasing with depth. The research by Grzelak et al. (2021) did not provide information on the total abundance of kinorhynchs including juveniles, so it cannot be compared, but the inclusion of them in the present study balances the results, blurring the pattern observed only with adults.

In terms of species richness, hadal trenches are characterized by a small number of species and a high number of endemism specific to each trench (Wolff, 1960; Belyaev, 1989; Eustace et al., 2016; Perrone et al., 2002). The Atacama Trench showed this same pattern in terms of the Kinorhyncha community, which was dominated by a single species collected only in this trench so far, *Echinoderes mamaqucha* (Grzelak et al., 2021). The South Orkney Trench shows a similar pattern, with the species *E. australis* sp. nov. dominating the whole community. In addition, densities of *E. australis* sp. nov. are higher at the hadal site, as was the case with *E. mamaqucha* in the Atacama Trench (Grzelak et al., 2021). Finally, it is worth mentioning that the Kinorhyncha community in the South Orkney Trench is not homogeneous, but varies with bathymetry, which has been seen previously in other trenches for meiofaunal organisms (Kitahashi et al., 2013; Leduc et al., 2016; Schmidt et al., 2019), including kinorhynchs (Grzelak et al., 2021). In this regard, the South Orkney Trench has higher diversity in the abyssal zone, inhabited by three echinoderm species, while only specimens of *E. australis* sp. nov. are present in the hadal depth. These results must be taken with caution due to the low number of samples included in the research as well as the reduced knowledge of kinorhynch diversity in the deep ocean in general and in trenches in particular.

4.5. Community structure of Kinorhyncha along the vertical profile in the South Orkney Trench

Regarding the distribution of the whole kinorhynch community along the sediment, the specimens are homogeneously distributed in the axis but unevenly in the terrace (concentrated up to 2 cm depth). This could be due to a higher oxygen availability in the deeper layers of the axis caused by bottom sea currents and bioturbation phenomenon of mega and macrofauna (Callaway, 2006). Our hypothesis is supported by the unusual abundance of macrofauna organisms found by Sokolova et al. (1996) in the bottom of the hadal zone of the South Orkney trench, at depths over 6.000 m.

The high proportion of juveniles compared to adults as well as the uneven distribution of juveniles along the vertical profile of the sediment has already been observed in previous studies (Álvarez-Castillo et al., 2015; Sánchez et al., 2022). The fact that only juveniles appear in the first sediment horizons while adults are found at greater depths, independent of the site, could be related to physical-chemical factors and the anatomy of the animals. It is well known that most meiofaunal organisms must inhabit at the first few centimetres of the sediment since the oxygen concentration decreases rapidly along the vertical profile of the seafloor (Higgins and Thiel, 1988; Sørensen and Pardos, 2020; Neuhaus, 2013). Considering that oxygen availability acts as a limiting factor for these organisms, we hypothesize that juveniles may have a greater oxygen demand due to a higher metabolic activity than adults, leading them to inhabit only the uppermost layers of the sediment. Another explanation would be related to a lesser development of juvenile anatomical structures involved in locomotion (Neuhaus, 2013). As the number of introvert structures increases in the ontogeny, juvenile stages would find it more difficult to move through the sediment particles of deeper, more compact layers, relegating these specimens to remain in the upper horizons.

CRediT authorship contribution statement

Nuria Sánchez: Writing – review & editing, Writing – original draft, Visualization, Investigation, Data curation, Conceptualization. **Marta García-Cobo:** Writing – review & editing, Visualization, Resources, Data curation. **Mauricio Shimabukuro:** Writing – review & editing, Visualization, Resources. **Daniela Zeppilli:** Writing – review & editing, Project administration, Funding acquisition. **Hidetaka Nomaki:** Writing – review & editing, Funding acquisition. **Alberto González-Casarrubios:** Writing – review & editing, Writing – original draft, Visualization, Investigation, Data curation.

Declaration of competing interest

González Casarrubios, Alberto reports that he has received financial support from the the International Seabed Authority's Sustainable Seabed Knowledge Initiative: One Thousand Reasons Campaign. Garcia Cobo, Marta reports that she has received financial support from the Erasmus+ short-term fellowships.

Acknowledgements

We thank the captains, crews, and the chief scientist Minoru Ikehara and onboard scientists of the cruise KH-19-6 "HEAW30: Integrated investigation for marine earth sciences in the Weddell Sea and the South Pacific: Fulfilment of R/V Hakuho-maru 30th anniversary expedition" of R/V Hakuho-maru. This work was partly supported by the Ocean Shot Research Grant Program "Massive mEIOfauna DiscoverY of new Species of our oceans and SEAs" (MEIODYSSEA) funded by the Sasakawa Peace Foundation (PI: Daniela Zeppilli) and the Danish National Research Foundation through the Danish Center for Hadal Research, HADAL (Grant number DNRF145). MGC was supported by an Erasmus+ short-term fellowship. Taxonomic research made by AGC and NS were supported by the International Seabed Authority's Sustainable Seabed Knowledge Initiative: One Thousand Reasons Campaign (co-financed by the European Maritime and Fisheries Fund of the European Union, Project 101071214 — SSKI-I — EMFAF-2021-ISA-SSKI-IBA). Finally, we would like to thank Martin V. Sørensen and Katarzyna Grzelak for their review of our manuscript, which contributed substantially to the improvement of the final version. Likewise, thanks to Martin V. Sørensen for the information provided on some structures of *Echinoderes* sp. 2 of the Atacama Trench and *Echinoderes angustus* deposited at the NHMD.

Appendix A. Supplementary data

Supplementary data to this article can be found online at https://doi.org/10.1016/j.jcz.2024.10.016.

Data availability

No data was used for the research described in the article.

References

Adrianov, A.V., Maiorova, A.S., 2019. *Echinoderes ultraabyssalis* sp. nov. From the Kuril-Kamchatka Trench – the first hadal representative of the Kinorhyncha (Kinorhyncha: Cyclorhagida). Prog. Oceanogr. 178, 102142. https://10.1016/j.pocean.2019.102142.

Álvarez-Castillo, L., Hermoso-Salazar, M., Estradas-Romero, A., Prol-Ledesma, R.M., Pardos, F., 2015. First records of Kinorhyncha from the Gulf of California: horizontal and vertical distribution of four genera in shallow basins with CO2 venting activity. Cah. Biol. Mar. 56 (3), 271–281.

Appeltans, W., Ahyong, S.T., Anderson, G., Angel, M.V., Artois, T., Bailly, N., et al., 2012. The magnitude of global marine species diversity. Curr. Biol. 22, 2189–2202. https://doi.org/10.1016/j.cub.2012.09.036.

Belyaev, G.M., 1989. Deep-sea Ocean Trenches and Their Fauna. Nauka Publishing House, Moscow, p. 255.

Callaway, R., 2006. Tube worms promote community change. Mar. Ecol. Prog. Ser. 308, 49–60. https://doi.org/10.3354/meps308049.

Carus, J.V., 1885. Prodromus Faunae Mediterraneae sive Descriptio Animalium maris Mediterranei incolarum quam comparata silva rerum quatenus innotiut adiectis et nominibus vulgaribus eorumque auctoribus in commodum zoologorum. Vol. I. Coelenterata, Echinodermata, Vermes, Arthropoda. E. Schweizerbartsche Verlagshandlung E. Koch, Stuttgart, p. 525.

Claparède, A.R.E., 1863. Beobachtungen über Anatomie und Entwicklungsgeschichte wirbelloser Thiere: an der Küste von Normandie angestellt. Verlag von Wilhelm Engelmann, Leipzig, pp. 1–120, 18 plates.

Danovaro, R., Della Croce, N., Dell'Anno, A., Pusceddu, A., 2003. A depocenter of organic matter at 7800m depth in the SE Pacific Ocean. Deep Sea Res. I 50, 1411–1420. https://doi.org/10.1016/j.dsr.2003.07.001.

Danovaro, R., Gambi, C., Della Croce, N., 2002. Meiofauna hotspot in the Atacama Trench, eastern South Pacific ocean. Deep Sea Res. I 49, 843–857. https://doi.org/10.1016/s0967-0637(01)00084-x.

Eustace, R.M., Kilgallen, N.M., Ritchie, H., Piertney, S.B., Jamieson, A.J., 2016. Morphological and ontogenetic stratification of abyssal and hadal *Eurythenes gryllus* (Amphipoda: Lysianassidae) from the Peru-Chile Trench. Deep-Sea Res., Part A I 109, 91–98. https://doi.org/10.1016/j.dsr.2015.11.005.

Fox, J., Weisberg, S., 2019. An R Companion to Applied Regression, third ed. Sage, Thousand Oaks CA.

Glover, A.G., Higgs, N., Horton, T., 2024. World register of Deep-Sea species (Words). Available from: https://www.marinespecies.org/deepsea. https://doi.org/10.14284/352. (Accessed 1 July 2024).

Glud, R.N., Berg, P., Thamdrup, B., Larsen, M., Stewart, H.A., Jamieson, J., et al., 2021. Hadal trenches are dynamic hotspots for early diagenesis in the deep sea. Commun. Earth Environ. 2, 21.

Glud, R.N., Wenzhöfer, F., Middelboe, M., Oguri, K., Turnewitsch, R., Canfield, D.E., et al., 2013. High rates of microbial carbon turnover in sediments in the deepest oceanic trench on Earth. Nat. Geosci. 6, 284–288. https://doi.org/10.1038/ngeo1773.

González-Casarrubios, A., Cepeda, D., Pardos, F., Neuhaus, B., Yamasaki, H., Herranz, M., Grzelak, K., Maiorova, A., Adrianov, A., Dal Zotto, M., Di Domenico, M., Landers, S.C., Sánchez, N., 2023. Towards a standardisation of morphological measurements in the phylum Kinorhyncha. Zool. Anz. 302, 217–223. https://doi.org/10.1016/j.jcz.2022.11.015.

González-Casarrubios, A., Pardos, F., Sørensen, M.V., Martínez Arbizu, P.M., Sánchez, N., 2022. *Dracophyes cepedai* gen. et sp. nov., a new Dracoderidae genus and species (Kinorhyncha: Allomalorhagida) from the Peru Basin. Zool. Anz. 301, 145–153. https://doi.org/10.1016/j.jcz.2022.10.004.

González-Casarrubios, A., Yamasaki, H., 2022. Kinorhyncha measurement database. Available from: https://sites.google.com/a/meiobenthos.com/laboratory/database/kinorhyncha-measurement-database. . (Accessed 1 July 2024).

Grzelak, K., Sørensen, M.V., 2018. New species of *Echinoderes* (Kinorhyncha: Cyclorhagida) from spitsbergen, with additional information about known arctic species. Mar. Biol. Res. 14 (2), 113–147. https://doi.org/10.1080/17451000.2017.1367096.

Grzelak, K., Sørensen, M.V., 2022. *Echinoderes* (Kinorhyncha: Cyclorhagida) from the Hikurangi Margin, New Zealand. Eur. J. Taxon. 844, 1–108. https://doi.org/10.5852/ejt.2022.844.1949.

Grzelak, K., Zeppilli, D., Shimabukuro, M., Sørensen, M.V., 2021. Hadal mud dragons: first insight into the diversity of Kinorhyncha from the Atacama Trench. Front. Mar. Sci. 8, 670735. https://doi.org/10.3389/fmars.2021.670735.

Grzelak, K., Yamasaki, H., Mincks, S., Phillips, A.J., Sørensen, M.V., 2023. Revision of an Arctic kinorhynch species: *Echinoderes svetlanae* and *E. tubilak* are junior synonyms of *E. remanei*. Zool. Anz. 302, 75–89. https://doi.org/10.1016/j.jcz.2022.11.001.

Harris, P.T., Macmillan-Lawler, M., Rupp, J., Baker, E.K., 2014. Geomorphology of the oceans. Mar. Geol. 352, 4–24. https://10.1016/j.margeo.2014.01.011.

Herranz, M., Stiller, J., Worsaae, K., Sørensen, M.V., 2022. Phylogenomic analyses of mud dragons (Kinorhyncha). Mol. Phylogenet. Evol. 168, 107375. https://doi.org/10.1016/j.ympev.2021.107375.

Higgins, R.P., Kristensen, R.M., 1988. Kinorhyncha from Disko Island, west Greenland. Smithsonian Contrib. Zool. 458, 1–56.

Higgins, R.P., Thiel, H., 1988. Introduction to the Study of Meiofauna. Smithsonian Institution Press, Washington D.C., p. 488

Jamieson, A.J., Fujii, T., Mayor, D.J., Solan, M., Priede, I.G., 2010. Hadal trenches: the ecology of the deepest places on Earth. Trends Ecol. Evol. 25, 190–197. https://doi.org/10.1016/j.tree.2009.09.009.

Janssen, A., Kaiser, S., Meißner, K., Brenke, N., Menot, L., Martínez Arbizu, P., 2015. A reverse taxonomic approach to assess macrofaunal distribution patterns in abyssal Pacific polymetallic nodule fields. PLoS One 10, e0117790. https://doi.org/10.1371/journal.pone.0117790.

Kitahashi, T., Kawamura, K., Kojima, S., Shimanaga, M., 2013. Assemblages gradually change from bathyal to hadal depth: a case study on harpacticoid copepods around the Kuril Trench (north-west Pacific Ocean). Deep Sea Res. I 74, 39–47. https://doi.org/10.1016/j.dsr.2012.12.010.

Leduc, D., Rowden, A.A., Glud, R.N., Wenzhöfer, F., Kitazato, H., Clark, M.R., 2016. Comparison between infaunal communities of the deep floor and edge of the Tonga Trench: possible effect of differences in organic matter supply. Deep Sea Res. I 116, 264–275. https://doi.org/10.1016/j.dsr.2015.11.003.

Lins, L., Zeppilli, D., Menot, L., Michel, L.N., Bonifacio, P., Brandt, et al., 2021. Toward a reliable assessment of potential ecological impacts of deep-sea polymetallic nodule mining on abyssal infauna. Limnol Oceanogr. Methods 19, 626–650. https://doi.org/10.1002/lom3.10448.

Neuhaus, B., 2013. Kinorhyncha (= Echinodera). In: Smith-Rhaesa, A. (Ed.), Handbook of Zoology. De Gruyter, Hamburg, pp. 181–349.

Neuhaus, B., Sørensen, M.V., 2013. Populations of *Campyloderes* sp. (Kinorhyncha, Cyclorhagida): one global species with significant morphological variation? Zool. Anz. 252 (1), 48–75. https://doi.org/10.1016/j.jcz.2012.03.002.

Pardos, F., Herranz, M., Sánchez, N., 2016. Two sides of a coin: the phylum Kinorhyncha in Panama. II) Pacific Panama. Zool. Anz. 265, 26–47. https://doi.org/10.1016/j.jcz.2016.06.006.

Perrone, F.M., Dell'Anno, A., Danovaro, R., Della Croce, N., Thurston, M.H., 2002. Population biology of *Hirondellea* sp. nov. (Amphipoda: Gammaridea: Lysianassoidea) from the Atacama Trench (south-east Pacific Ocean). J. Mar. Biol. Assoc. 82, 419–425. https://doi.org/10.1017/s0025315402005672.

Sánchez, N., González-Casarrubios, A., Cepeda, D., Khodami, S., Pardos, F., Vink, A., Martínez Arbizu, P., 2022. Diversity and distribution of Kinorhyncha in abyssal polymetallic nodule areas of the Clarion-Clipperton Fracture Zone and the Peru Basin, East Pacific Ocean, with the description of three new species and notes on their intraspecific variation. Mar Biodiversity 52, 52. https://doi.org/10.1007/s12526-022-01279-z.

Schmidt, C., Martínez Arbizu, P., 2015. Unexpectedly higher metazoan meiofauna abundance in the Kuril-Kamchatka trench compared to the adjacent abyssal plains. Deep Sea Res. II: Top. Stud. Oceanogr. 111, 60–75. https://doi.org/10.1016/j.dsr2.2014.08.019.

Schmidt, C., Sattarova, V.V., Katrynski, L., Martìnez Arbizu, P., 2019. New insights from the deep: meiofauna in the Kuril-Kamchatka Trench and adjacent abyssal plain. Prog. Oceanogr. 173, 192–207. https://doi.org/10.1016/j.pocean.2019.02.010.

Shimabukuro, M., Zeppilli, D., Leduc, D., Wenzhöfer, F., Berg, P., Rowden, A.A., Glud, R.N., 2022. Intra-and inter-spatial variability of meiofauna in hadal trenches is linked to microbial activity and food availability. Sci. Rep. 12 (1), 4338. https://doi.org/10.1038/s41598-022-08088-1.

Sokolova, M.N., Vinogradova, N.G., Burmistrova, I.I., 1996. «Rain of dead bodies» as a source of food for the ultra-abyssal macrobenthos in the Orkney trench. Oceanol. 35 (4), 539–543.

Somerfield, P.J., Warwick, R.M., 1996. Meiofauna in Marine Pollution Monitoring Programmes: A Laboratory Manual. Ministry of Agriculture, Fisheries and Food, Directorate of Fisheries Research, Lowestoft, Suffolk, p. 71.

Sørensen, M.V., Dal Zotto, M., Rho, H.S., Herranz, M., Sánchez, N., Pardos, F., Yamasaki, H., 2015. Phylogeny of Kinorhyncha based on morphology and two molecular loci. PLoS One 10 (7), e0133440. https://doi.org/10.1371/journal.pone.0133440.

Sørensen, M.V., Pardos, F., 2020. Kinorhyncha. In: Smith-Rhaesa, A. (Ed.), Guide to the Identification of Marine Meiofauna. Verlag Dr. Friedrich Pfeil, Munich, pp. 391–415.

Sørensen, M.V., Rohal, M., Thistle, D., 2018. Deep-sea Echinoderidae (Kinorhyncha: Cyclorhagida) from the Northwest Pacific. Eur. J. Taxon. 456, 1–75. https://doi.org/10.5852/ejt.2018.456.

Stewart, H.A., Jamieson, A.J., 2018. Habitat heterogeneity of hadal trenches: considerations and implications for future studies. Prog. Oceanogr. 161, 47–65. https://doi.org/10.1016/j.pocean.2018.01.007.

United Nations Educational, Scientific and Cultural Organization (UNESCO), 2009. Global Open Oceans and Deep Seabed (GOODS). Biogeographic Classification. Intergovernmental Oceanographic Commission. IOC Technical Series No. 84. UNESCO-IOC, Paris.

Vinogradova, N.G., Belyaev, G.M., Gebruk, Andrey, Zhivago, A.V., Kamenskaya, O., Levitan, M.A., Romanov, V.N., 1993. The studies of the Orkney Trench during cruise 43 of R/V Dmitrii Mendeleev. Tr. IO RAN 127, 9–33.

Watling, L., Guinotte, J., Clark, M.R., Smith, C.R., 2013. A proposed biogeography of the deep ocean floor. Prog. Oceanogr. 111, 91–112. https://doi.org/10.1016/j.pocean.2012.11.003.

Wenzhöfer, F., Oguri, K., Middelboe, M., Turnewitsch, R., Toyofuku, T., Kitazato, H., et al., 2016. Benthic carbon mineralization in hadal trenches: assessment by in situ O2 microprofile measurements. Deep Sea Res. I 116, 276–286. https://doi.org/10.1016/j.dsr.2016.08.013.

Wolff, T., 1960. The hadal community, an introduction. Deep Sea Res. 6, 95–124. https://doi.org/10.1016/0146-6313(59)90063-2.

WoRMS Editorial Board, 2024. World register of Marine species. Available from: https://www.marinespecies.orgatVLIZ. https://doi.org/10.14284/170. (Accessed 22 July 2024).

Xu, Y., Li, X., Luo, M., Xiao, W., Fang, J., Rashid, H., Peng, Y., Li, W., Wenzhöfer, F., Rowden, A.A., Glud, R.N., 2021. Distribution, source, and burial of sedimentary organic carbon in Kermadec and Atacama Trenches. J. Geophys. Res.-Biogeo. 126 (5). https://doi.org/10.1029/2020JG006189.

Yamasaki, H., Grzelak, K., Sørensen, M.V., Neuhaus, B., George, K.H., 2018a. *Echinoderes pterus* sp. n. showing a geographically and bathymetrically wide distribution pattern on seamounts and on the deep-sea floor in the Arctic Ocean, Atlantic Ocean, and the Mediterranean Sea (Kinorhyncha, Cyclorhagida). ZooKeys 771, 15–40. https://doi.org/10.3897/zookeys.771.25534.

Yamasaki, H., Herranz, M., Sørensen, M.V., 2020. An interactive identification key to species of Echinoderidae (Kinorhyncha). Zool. Anz. 287, 14–16. https://doi.org/10.1016/j.jcz.2020.05.002.

Yamasaki, H., Neuhaus, B., George, K.H., 2018b. Three new species of Echinoderidae (Kinorhyncha: Cyclorhagida) from two seamounts and the adjacent deep-sea floor in the Northeast Atlantic Ocean. Cah. Biol. Mar. 59, 79–106. https://doi.org/10.21411/CBM.A.124081A9.

Yamasaki, H., Neuhaus, B., George, K.H., 2019. Echinoderid mud dragons (Cyclorhagida: Kinorhyncha) from Senghor Seamount (NE Atlantic Ocean) including general discussion of faunistic characters and distribution patterns of seamount kinorhynchs. Zool. Anz. 282, 64–87. https://doi.org/10.1016/j.jcz.2019.05.018.

Zelinka, C., 1896. Demonstration der Tafeln der Echinoderes-Monographie. Verh. Dtsch. Zool. Ges. 6, 197–199.